Intrachain polaron motion and geminate combination in donor-acceptor copolymers: Effects of level offset and interfacial coupling

Yuan Li,[1] Kun Gao,[1] Zhen Sun,[1] Sun Yin,[1] De-sheng Liu,[1,2,*] and Shi-jie Xie[1]
[1]*School of Physics, State Key Laboratory of Crystal Materials, Shandong University, Jinan 250100, China*
[2]*Department of Physics, Jining University, Qufu 273155, China*
(Received 27 February 2008; published 31 July 2008)

A model study of polaron motion and geminate combination in a molecular chain of donor-acceptor copolymers is presented. The simulations are performed within the framework of an extended version of the one-dimensional Su-Schrieffer-Heeger tight-binding model. Two effects are mainly concerned: One is level offset, and the other is interfacial coupling. A general rule associated with the ratio of level offset to polaron or exciton binding energy is obtained to contribute to optimizing donor-acceptor copolymers for optoelectronic applications. According to the rule, we identify two cases for polaron motion and four cases for geminate combination of oppositely charged polarons. It is found that an interface with weak coupling serves as an energy barrier and that with strong coupling as a well, both of which can significantly affect the intrachain process in copolymers. The effect of electron-electron interaction is briefly discussed.

DOI: 10.1103/PhysRevB.78.014304 PACS number(s): 71.38.−k, 72.80.Le, 71.35.−y

I. INTRODUCTION

Photophysical researches and applications of conjugated polymers, such as organic light-emitting diodes (LEDs),[1] organic field-effect transistors,[2] and photovoltaic cells,[3] have received increasing attention in physics, chemistry and material science. An effective strategy for enhancing device efficiency is to employ copolymers instead of homopolymers as active components.[4–11] Copolymers can enhance the photo- and electroluminescent efficiency of LEDs by increasing conductivities of both electrons and holes and by interfacial confinement of excitons.[5–8] On the other hand, efficient photoinduced charge transfer and separation for photovoltaic applications can also be obtained by donor-acceptor copolymers.[9–11] Furthermore, the functionality of copolymers can be easily tailored by chemical synthesis, molecular design and self-assembly to make suitable for a particular application.[12–14]

It is known that the microcosmic electronic behavior in polymers mainly involves interchain and intrachain processes. In films or phase-separated blends of samples, interchain process dominates between neighboring molecular chains of parallel alignment, such as polaron hopping,[15,16] photoinduced charge separation,[17,18] and exciton dissociation.[19,20] In samples in dilute solutions or with ordered self-assembly phase,[21,22] intrachain process, e.g., polaron drift,[23–25] intramolecular charge transfer[26,27] and carriers recombination,[28,29] mainly occurs in a single chain. A detailed understanding of charge-carrier and exciton related behaviors and mechanisms in polymers is of great significance for application.

A recent work by Bittner *et al.*[30] studied theoretically the interchain process of exciton dissociation in various donor-acceptor polymers by considering two parallel chains of heterogeneity. It was found that when the exciton binding energy is greater than the band offset of the two chains, the exciton will remain stable and the polymer will make efficient LEDs. On the other hand, if the band offset is greater than the exciton binding energy, the exciton will fiss to form interchain charge-separated states and the polymer will be suitable for photovoltaic applications. It suggests that the ratio of band offset to the exciton binding energy is effective in guiding experiments to optimize polymers to meet LEDs or photovoltaic needs. One can expect that in an analogous system of donor-acceptor copolymers, the interchain process between donor and acceptor segments of adjacent chains should obey a similar rule. However, a straightforward extension to the intrachain process is invalid owing to distinct electronic and lattice behaviors. We expect that a more general rule associated with the behaviors of polarons and excitons can be obtained if two issues at least are addressed in the intrachain process of donor-acceptor copolymers.

In the first place, exciton binding energy in polymers, e.g., poly(phenylenevinylene) (PPV), is under intense debate as its magnitude is reported experimentally ranging from 25 meV to 1 eV.[31–36] The debate arises from various aspects and one of the most important problems is the definition of exciton binding energy. With regard to this issue, Conwell[37] suggested in the long chain limit an unambiguous definition of exciton binding energy. It was taken in two forms as the difference between the energy gap or the "single-particle energy gap"[35] and the optical-absorption edge. The former definition holds if an exciton dissociates into a free electron and a hole, while the latter is valid if it fisses to create a pair of oppositely charged polarons. In the study in Ref. 30, only the latter definition is adopted. We claim that, however, for the intrachain process in copolymers, both definitions are important for an exciton.

In the second place, the donor-acceptor interfaces for interchain and intrachain processes are markedly different. The interchain interface is formed by nearly fixed coupling between counterpart lattice sites of two parallel chains with hopping energy about 1 order of magnitude smaller than that of the intrachain hopping. However, the intrachain interface is usually a flexible covalent bond joining the end sites of the donor and the acceptor segments. Extra electrons or holes can change the bond as a result of the strong electron-lattice coupling in copolymers. Furthermore, the interfacial hopping

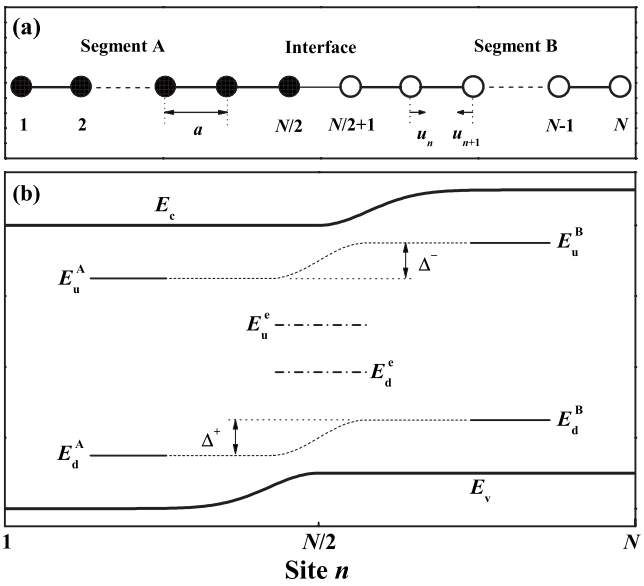

FIG. 1. Schematic diagram of (a) the lattice sites and (b) the energy levels in the gap of a molecular chain of donor-acceptor copolymer. E_c (E_v) represents the bottom (top) of the conduction (valence) band, and the rest of the conduction (valence) band is omitted. The solid lines E_u^A (E_u^B) and E_d^A (E_d^B) are localized energy levels for a polaron created in segment A (B). The short dashed lines represent the continuous energy variation of a polaron moving from segment A (B) to segment B (A), and Δ^- (Δ^+) is the energy-level offset of an electron (hole) polaron. The dashed-dotted lines E_u^e and E_d^e are localized energy levels for an exciton created at the interface. Other symbols are given in the text.

integral can also be affected by the degree of π-electron overlap between the donor and the acceptor segments at the interface. It can be attributed to the effect of torsion angle between the two segments in a twisted copolymer chain. The ring torsion angle in polymers, e.g., PPV, has been demonstrated to have a strong effect on the intrachain charge-carrier mobility.[38] Thus, the interfacial coupling effects should be considered for intrachain process in copolymers.

In this paper, by simulating the dynamic processes of intrachain polaron motion and geminate combination, we derive a general rule that helps to optimize donor-acceptor copolymers for optoelectronic applications. The rule is associated with the ratio of the level offset between the donor and the acceptor segments to polaron or exciton binding energy. The effect of interfacial coupling on the processes is also analyzed. The paper is organized as follows: The model and method are presented in Sec. II and the results and discussions are shown in Sec. III. Finally, summary and concluding remarks are given in Sec. IV.

II. MODEL AND METHOD

We consider a molecular chain of copolymers consisting of two homopolymer segments with a donor-acceptor-type electronic structure, as shown schematically in Fig. 1. The two segments, labeled separately A and B, are attached at the ends through a covalent bond. The system can be described by an extended version of the one-dimensional Su-Schrieffer-Heeger (SSH) tight-binding model.[39,40] The Hamiltonian consists of three parts.

$$H = H_e + H_f + H_l, \tag{1}$$

where H_e is the electronic part of the system.

$$H_e = \sum_n \Delta_n c_n^\dagger c_n - \sum_n t_{n,n+1}(c_{n+1}^\dagger c_n + \text{H.c.}). \tag{2}$$

The effect of external electric field is described in the Coulomb gauge with a scalar potential and the dipole approximation

$$H_f = eF\sum_n (na + u_n)(c_n^\dagger c_n - 1) \tag{3}$$

and

$$H_l = \frac{K}{2}\sum_n (u_{n+1} - u_n)^2 + \frac{M}{2}\sum_n \dot{u}_n^2 \tag{4}$$

describes the classical treatment of the elastic potential and kinetic energy of the lattice.

Here, Δ_n denotes the on-site energy of π-electrons on site n, $c_n^\dagger$ (c_n) the creation (annihilation) operator of an electron at site n, a the average lattice spacing, u_n the displacement of site n, F the electric field, K the elastic constant, and M the mass of a site.

The transfer integral $t_{n,n+1}$ between site n and site $n+1$ reads

$$t_{n,n+1} = t_0 - \alpha(u_{n+1} - u_n) - t' \cos(n\pi/2), \tag{5}$$

where t_0 represents the nearest-neighbor transfer integral for an undimerized lattice, α the electron-lattice coupling constant, and t' a symmetry-breaking parameter introduced to remove the ground-state degeneracy. The factor $\cos(n\pi/2)$ describes the molecular monomer consisting of multisites in the chain direction. This reflects the lattice feature of many widely used conjugated polymers, such as polythiophen, poly(p-phenylene) and PPV.[40–42]

The interfacial coupling is described by a dimensionless parameter β. The transfer integral at the interface separating segment A from B is given by

$$t_{N/2,N/2+1} = \frac{\beta}{2}(t^A_{N/2,N/2+1} + t^B_{N/2,N/2+1}), \tag{6}$$

where N is the total number of sites.

The evolution of the electrons depends on the time-dependent Schrödinger equation

$$i\hbar\partial_\tau|\Phi_\nu(\tau)\rangle = \left[H_e + eF\sum_n (na + u_n)c_n^\dagger c_n\right]|\Phi_\nu(\tau)\rangle, \tag{7}$$

and the development of lattice displacements is classically described by the Newtonian equation of motion

$$M\ddot{u}_n = -K(2u_n - u_{n+1} - u_{n-1}) + 2\alpha[\rho_{n,n+1}(\tau) - \rho_{n-1,n}(\tau)] + eF[\rho_{n,n}(\tau) - 1] - \lambda M\dot{u}_n. \tag{8}$$

The density matrix $\rho_{n,m}(\tau)$ is given by

$$\rho_{n,m}(\tau) = \sum_{\nu} \Phi^{*}_{\nu,n}(\tau) f_{\nu} \Phi_{\nu,m}(\tau) \tag{9}$$

and $\Phi_{\nu,n}(\tau) = \langle n | \Phi_{\nu}(\tau) \rangle$ is the projection of electronic state $|\Phi_{\nu}(\tau)\rangle$ on the Wannier state of site n. f_{ν} denotes the time-independent occupation function of state $|\Phi_{\nu}(\tau)\rangle$ and is solely determined by the initial occupation (0, 1 or 2). A damping term is introduced in Eq. (8) to describe the energy dissipation into the surrounding medium by a tuning parameter λ.[24]

For any given time, the electronic state $|\Phi_{\nu}(\tau)\rangle$ can be expanded on the basis of instantaneous eigenstates

$$|\Phi_{\nu}(\tau)\rangle = \sum_{\mu} C_{\nu,\mu}(\tau) |\phi_{\mu}(\tau)\rangle, \tag{10}$$

where $C_{\nu,\mu}(\tau) = \langle \phi_{\mu}(\tau) | \Phi_{\nu}(\tau) \rangle$ and $\{|\phi_{\mu}(\tau)\rangle\}$ are eigensolutions to the Schrödinger equation

$$H_{e} |\phi_{\mu}(\tau)\rangle = \varepsilon_{\mu}(\tau) |\phi_{\mu}(\tau)\rangle \tag{11}$$

at a given instant τ. The Hamiltonian is determined by the instantaneous lattice positions $\{u_n(\tau)\}$. Note that $C_{\nu,\mu}(\tau=0) = \delta_{\nu,\mu}$. The occupation number of the instantaneous eigenstate $|\phi_{\mu}(\tau)\rangle$ is

$$n_{\mu}(\tau) = \sum_{\nu} f_{\nu} C^{2}_{\nu,\mu}(\tau). \tag{12}$$

Here $n_{\mu}(\tau)$ is allowed to change and reflects a nonadiabatic effect of the redistribution of electrons among the instantaneous eigenstates.[43] The coupled differential Eqs. (7) and (8) are solved by the Runge-Kutta method of order 8 with step-size control.[44] It has been widely used and proven to be an effective approach in the study of dynamics in conjugated polymers.[24,25,43,45]

The molecular chain contains $N=200$ sites, with segment A and B 100 sites, respectively. Before the dynamics, a static chain is constructed with 200 π-electrons doubly occupying the 100 levels of the valence band. Adding (Removing) an electron to (from) the 101st (100th) level at the bottom (top) of the conduction (valence) band, an electron (hole) polaron is created in segment A (B) by iteratively solving the static electronic eigenequation [Eq. (13)] and the lattice balance equation [Eq. (14)].

$$\Delta_n \phi_{\mu,n} - t_{n-1,n} \phi_{\mu,n-1} - t_{n,n+1} \phi_{\mu,n+1} = \varepsilon_{\mu} \phi_{\mu,n} \tag{13}$$

$$u_{n+1} - u_n = -\frac{2\alpha}{K} \left(\rho_{n,n+1} - \frac{1}{N-1} \sum_{m} \rho_{m,m+1} \right) \tag{14}$$

Here $\phi_{\mu,n} = \Phi_{\mu,n}(\tau=0)$ and $\rho_{n,n+1} = \rho_{n,n+1}(\tau=0)$. The balance equation is obtained by minimizing the total energy E of the system, i.e., $\partial E / \partial u_n = 0$. The total energy consists of the electronic energy and the elastic potential energy of the lattice.

$$E = \sum_{\mu} \varepsilon_{\mu} f_{\mu} + \frac{K}{2} \sum_{n} (u_{n+1} - u_n)^2 \tag{15}$$

Starting from the initial state given by Eqs. (13) and (14), the system will evolve by obeying Eqs. (7) and (8).

The values of parameters in the Hamiltonian for both segments A and B are chosen to be those generally used for polymers:[39,40] $t_0 = 2.5$ eV, $t' = 1.0$ eV, $\alpha = 4.5$ eV/Å, $K = 21.0$ eV/Å^2, $a = 1.22$ Å, and $M = 1349.14$ eV fs^2/Å^2. To obtain a donor-acceptor-type electronic structure in the molecular chain, we set different values to the on-site energy of segments A and B: $\Delta_n^{A} = 0$, $\Delta_n^{B} = \Delta$, where Δ is chosen in connection with the results given in Sec. III. Then we obtain level offsets, or polaronic level offsets, at the interface: $\Delta^{-} = \Delta^{+} = \Delta$, as shown in Fig. 1(b). The damping parameter is chosen as $\lambda = 1.0 \times 10^{-3}$ fs^{-1}.[24] To avoid numerical errors, the electric field F is turned on smoothly within the first 50 fs and then maintained constant. A time step of $\Delta\tau = 1$ fs is chosen and a fixed-end boundary condition is proposed.

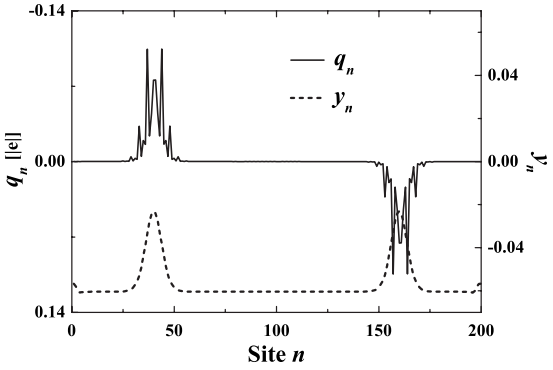

FIG. 2. Net charge distribution q_n and static lattice configuration y_n of a molecular chain with two oppositely charged polarons. The unit of y_n is in angstrom.

III. RESULTS AND DISCUSSIONS

According to the procedure given in Sec. II, one can construct a single polaron or a pair of oppositely charged polarons as sufficiently separated as possible in the molecular chain. A polaron can be purposely located in the chain by setting an initial condition of polaron lattice configuration with fixed position to Eq. (13) at the beginning of the iteration.[46] A chain with two oppositely charged polarons is shown in Fig. 2, where $q_n = e(\rho_{n,n} - 1)$ is the net charge distribution on site n and $y_n = (2\delta_n + \delta_{n+1} + \delta_{n-1})/4$ is the smoothed lattice order parameter with $\delta_n = (-1)^n (u_{n+1} - u_n)$ the lattice distortion between site n and site $n+1$. The polarons, about 25 sites in width, are constructed in the large polaron limit with the electronic charge and the localized lattice deformation coupled together. An electron polaron with negative net charge is prone to be created in segment A, while a hole polaron with positive net charge favors to reside in segment B, reflecting the feature of the donor-acceptor electronic structure. As the effect of electron-electron (e-e) interaction is not included here, the singlet and triplet states of the molecule have the same energy and are not distinguishable in the present model.

Before the study of our interest, it is crucial to check for the stability of the constructed polarons. An effective approach is to evaluate the strength of the dissociation electric field over which a polaron dissociates into a free charge. To this end, we study the motion of a polaron driven by strong electric field in a chain without level offset. It is found that

for fields over about 1.5×10^6 V/cm, the polaron begins to move unstably and dissociates eventually after some distance. With fields up to about 2.0×10^6 V/cm, the polaron breaks down quickly as soon as the field is applied, in accordance with the description of polaron dissociation in Ref. 23 where this issue was detailedly addressed. As the model considered here is a perfect chain without defects induced by, e.g., impurities or thermal fluctuations, the stability of a polaron is mainly determined by the electric field. Consequently, the polaron is stable enough for fields below the range of dissociation field in the study here in polaron regime. In addition, it has been demonstrated that the dissociation field is nearly proportional to the polaron binding energy in the large polaron limit.[47] A given polaron holds a fixed binding energy while the dissociation field is within a range. It is more convenient to employ polaron binding energy to describe the stability of a polaron in the following study.

In the dynamics, we mainly focus on the time evolution of the net charge distribution Q_n. It is defined as the smoothed form of q_n, i.e., $Q_n=(2q_n+q_{n+1}+q_{n-1})/4$, to rule out artifacts. The development of y_n is also presented when necessary.

A. Polaron motion

The motion of a polaron driven by external electric field is studied. An electron polaron is initially centered in segment A around the 40th site to the left end of the chain. The impact of level offset on polaron motion is first studied and then the interfacial coupling effect is considered.

1. Effect of level offset

An effective parameter describing polaron stability is polaron binding energy ε_b^p, defined as the energy gain of a polaron in the dissociation process.[48] The polaron binding energy is crucial for charge transport in organic samples, e.g., DNAs, disordered organic solids, and copolymers, where polaron effects are important.[49–51] In the present model, the binding energy of an electron (hole) polaron is given by

$$\varepsilon_b^{p^{-(+)}} = E_1^{p^{-(+)}} - E_0^{p^{-(+)}}, \tag{16}$$

where $E_0^{p^{-(+)}}$ and $E_1^{p^{-(+)}}$ is the total energy of a chain before and after the dissociation of the polaron, respectively. With parameters in Sec. II, we obtain that the polaron binding energy is $\varepsilon_b^p=0.16$ eV. It is clearly seen from Fig. 1(b) that the level offset at the interface is a barrier with height Δ^- for an electron polaron moving from segment A to B. We then set values based on the polaron binding energy to the level offset in the study below. The interfacial coupling parameter is chosen $\beta=1$ as an average coupling.

a. $\Delta<\varepsilon_b^p$. We present in Fig. 3 the evolution of Q_n for different cases. For a chain with level offset of $\Delta=0.1$ eV, less than the polaron binding energy, the behavior of a polaron is shown in Figs. 3(a) and 3(b). At an electric field below 7.2×10^5 V/cm, the polaron moves steadily in segment A but gets stuck at the interface for the blockage of the level offset [see Fig. 3(a)]. By increasing slightly the field strength, e.g., up to 7.3×10^5 V/cm, the polaron remains at the interface for about 60 fs requiring enough energy to eventually overcome the blockage and continues its motion in segment B [see Fig. 3(b)]. It is evident that there exists a threshold electric field F_{th} over which the polaron moves steadily beyond the interface for a fixed level offset. More calculations for different level offsets within $\Delta<\varepsilon_b^p$ give similar results.

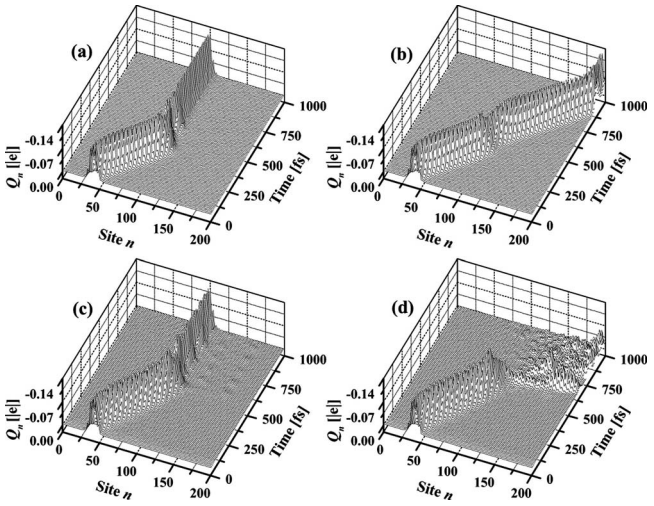

FIG. 3. Time dependence of Q_n of a polaron in a chain with (a) $\Delta=0.1$ eV, $F=7.2\times10^5$ V/cm; (b) $\Delta=0.1$ eV, $F=7.3\times10^5$ V/cm; (c) $\Delta=0.2$ eV, $F=1.54\times10^6$ V/cm; (d) $\Delta=0.2$ eV, $F=1.55\times10^6$ V/cm.

b. $\Delta>\varepsilon_b^p$. By increasing the level offset up to magnitudes greater than the polaron binding energy, one can obtain a different case. In Figs. 3(c) and 3(d), the level offset is chosen as $\Delta=0.2$ eV. It is found that for fields below about 1.54×10^6 V/cm, the behavior of a polaron resembles the case in Fig. 3(a). Even for the field of 1.54×10^6 V/cm, though within the range of dissociation field, the polaron is stable on the whole at the interface but with a little charge tunneling into segment B [see Fig. 3(c)]. However, for fields up to and greater than 1.55×10^6 V/cm, the polaron dissociates directly with the charge crossing the interface [see Fig. 3(d)] but the lattice deformation broken down (not shown). It is clear that there exists a critical electric field below which the motion of a polaron is hindered by the interface while over which the polaron dissociates. Similar behaviors are also observed for other values of level offset greater than the polaron binding energy. The polaron dissociation here is intrinsic as the critical field is independent of the increase in the level offset. It is understood that the polaron is not stable enough to overcome the level offset and cannot survive under sufficiently strong electric fields.

It should be mentioned that the polaron binding energy used in some studies with the same tight-binding method is approximately defined as the energy difference between the polaron level and the closest band edge.[52,53] With this definition, it is about $\varepsilon_b^p=0.39$ eV in the present model. However, it is inadequate to simply employ this magnitude of polaron binding energy for the study here. For instance, for a level offset between 0.16 eV and 0.39 eV, the "polaron bind-

ing energy" is greater than the interfacial barrier but the polaron is not stable enough to get across the interface. It is obviously unbelievable in the absence of other effects, e.g., the interfacial coupling that will be discussed below. This mainly arises from the fact that the approximate definition refers to only the electronic energy but excludes the elastic potential energy of the lattice. For the polaron dynamics here, in which both the charge and the lattice take part in the transport, it is certainly more reasonable to employ polaron binding energy calculated by the total energy of the system including both the electronic and the lattice part.

Therefore, based on the analysis, a rule determining intrachain polaron motion in the copolymers can be derived. If the polaron binding energy is greater than the level offset, a polaron can cross the interface only if the electric field is strong enough. Otherwise, the polaron, as an entity consisting of both charge and lattice deformation, cannot cross the interface regardless of the strength of electric field. One can expect that the blockage of interface does not work well if the carriers are free charges beyond the polaron regime. Experimentally, it was found that a copolymer synthesized from homopolymers of distinct electronic structures with level offset much greater than the magnitude of polaron binding energy, e.g., a pyrrole-aniline copolymer,[54] generally exhibits a reduced conductivity as compared to that of the homopolymers. In contrast, however, a highly conductive copolymer can be prepared by the copolymerization of a homopolymer and its substituted derivatives, e.g., an aniline copolymer containing butylthio substituent,[55] where the segments are of band similarity. It is expected that the level or band offset between different segments of the copolymers plays an important role in affecting the transport of charge carriers therein, though the presence of other effects may also work.

2. *Effect of interfacial coupling*

We now consider the effect of interfacial coupling. In the present model, $\beta > 1$ is referred to as a strong coupling and $\beta < 1$ as a weak one. We depict in Fig. 4 the dependence of threshold electric field F_{th} on β for a polaron that moves in a chain with $\Delta = 0.1$ eV. For both weak and strong couplings, the threshold electric field for a polaron to overcome the interface is higher than that for the average coupling. The tunable range of β is from 0.95 to 1.08. Any magnitude of β outside this range results in the dissociation of the polaron before it gets across the interface.

By examining the variation of the interfacial bond length, it is found that the bond length decreases with the increase in β. For weak coupling, the bonding between the two segments weakens. It is equivalent to an "energy barrier" created at the interface by adding Δ_{add} to the original level offset, as shown schematically in the inset of Fig. 4. Thus the polaron transition from segment A into B becomes more difficult. For strong coupling, one might expect that with the strengthening of the bonding between the two segments, the additional energy barrier would be lower and the polaron would cross the interface more easily. However, this is not the case. The interface with strong coupling serves not as a barrier but as a well in which the polaron is easily trapped, also shown schematically in the inset of Fig. 4. An additional energy Δ_{add} is introduced to form an asymmetric well and then the right-hand wall of the well lifts the effective level offset barrier.

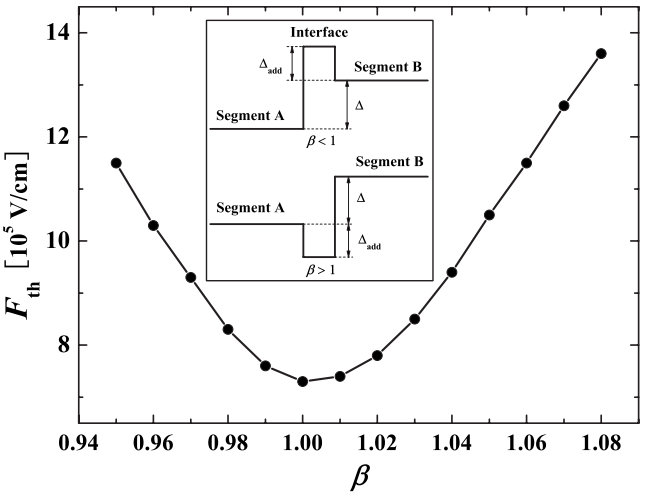

FIG. 4. The threshold electric field F_{th} of a polaron versus β in a chain with level offset of $\Delta = 0.1$ eV. The inset is a schematic diagram of the effect of interfacial coupling.

To confirm this analysis, we study the motion of a polaron in a chain without level offset. The electric field is switched off before the polaron encounters the interface so as to eliminate the effect of electric field hereafter. The result is shown in Fig. 5. For $\beta = 0.9$ the polaron rebounds from the interface while for $\beta = 1.1$ it is trapped by interface electronic states, in accordance with our expectation. This behavior is entirely determined by the effect of interfacial coupling in the absence of level offset and electric field. Therefore, it can be concluded that the interfacial coupling can be as important as level offset in impacting on the polaron motion in donor-acceptor copolymers.

B. Geminate combination of polarons

We further study the dynamics of two oppositely charged polarons which encounter and combine geminately at the interface of the copolymers under the influence of electric field. Initially, in addition to an electron polaron in segment A, a hole polaron is symmetrically centered in segment B

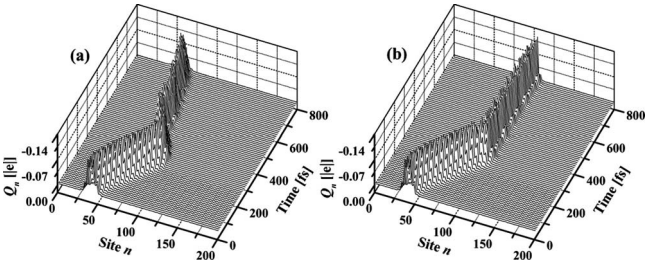

FIG. 5. Time dependence of Q_n of a polaron in a chain with (a) $\beta = 0.9$; (b) $\beta = 1.1$. The level offset is $\Delta = 0$. The electric field is $F = 1.0 \times 10^6$ V/cm and is switched off at $\tau = 250$ fs.

around the 40th site to the right end of the chain.

1. Effect of level offset

We focus on the effect of level offset by setting $\beta=1$. Referring to Ref. 37, we define the exciton binding energy in two forms: ε_b^{eI} and ε_b^{eII}. Supplying an exciton with energy ε_b^{eI} gives rise to the creation of a pair of oppositely charged polarons, while with energy ε_b^{eII} dissociates it into a free electron and a hole. They are given by

$$\varepsilon_b^{eI} = E_I^e - E_0^e \tag{17}$$

and

$$\varepsilon_b^{eII} = E_{II}^e - E_0^e, \tag{18}$$

respectively. Here E_0^e is the total energy of a chain with an exciton, E_I^e is that with a pair of oppositely charged polarons far away enough from each other, and E_{II}^e is that with a fully separated electron-hole pair.

In calculations, E_I^e and E_{II}^e can be further represented as

$$E_I^e = E_0^{p^-} + E_0^{p^+} - E_0 \tag{19}$$

and

$$E_{II}^e = E_I^{p^-} + E_I^{p^+} - E_0, \tag{20}$$

where E_0 is the total energy of the chain in ground state. Combining Eqs. (16)–(20), we obtain an important relation,

$$\varepsilon_b^{eI} + \varepsilon_b^{p^-} + \varepsilon_b^{p^+} = \varepsilon_b^{eII}. \tag{21}$$

This reflects the conservation of energy in the two ways of dissociating an exciton into a pair of free charges. With parameters in Sec. II, we obtain $\varepsilon_b^{eI}=0.47$ eV and $\varepsilon_b^{eII}=0.79$ eV. By setting values to the level offset based on ε_b^p, ε_b^{eI} and ε_b^{eII}, we identify four cases for the geminate combination.

a. $\Delta < \varepsilon_b^p$. The behavior of a pair of polarons in a chain with level offset of $\Delta=0.1$ eV is depicted in Fig. 6. The level offset is less than the polaron binding energy. It is found that this process is field dependent.

For a relatively weak electric field, e.g., 5.0×10^5 V/cm, the two polarons collide at the interface, pass through each other and then continue moving in the same direction with just a lower velocity and less amount of net charge, as shown in Fig. 6(a). For the lattice development shown in Fig. 6(c), it seems that, however, the two polarons rebound rather than pass through after the collision as no evident overlap and enhancement of the polaron deformations at the time of collision is observed. This paradoxical behavior will be explained later by analyzing the energy levels.

For a strong field, such as 1.0×10^6 V/cm, the two polarons collide twice in succession and eventually merge at the interface into a single deformation. This behavior is clearly depicted in the development of the lattice in Fig. 6(d). From the evolution of the net charge distribution, as shown in Fig. 6(b), one can see that the net charge amount of the two polarons greatly decreases after the first collision and nearly vanishes after the successive second collision. Simultaneously, however, a slight net charge fluctuation on the chain is widely induced.

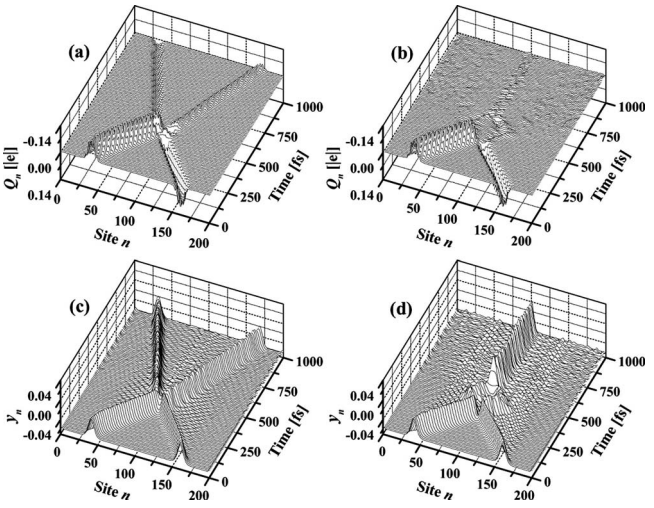

FIG. 6. Time dependence of Q_n and y_n of two oppositely charged polarons in a chain with level offset of $\Delta=0.1$ eV under electric fields: (a), (c) $F=5.0\times10^5$ V/cm; (b), (d) $F=1.0\times10^6$ V/cm. The unit of y_n is in angstrom.

The different behaviors can be understood by analyzing the energy levels. We present in Fig. 7 the evolution of the instantaneous eigenlevels and their occupation number. Level 99 (100) and level 101 (102) are localized levels for the electron (hole) polaron in segment A (B). Level 98 and level 103 are delocalized levels in the continuum near the gap. One can see from the insets of Figs. 7(a) and 7(b) that the occupation number of the polaron levels changes during the collision. It indicates that electron transition occurs between the two polarons. It can be understood in this way. If the level offset vanishes, the counterpart levels of the two polarons, e.g., level 99 and level 100, are actually degenerate. A level offset of 0.1 eV eliminates the degeneracy to some extent but hardly prevents the wave functions from overlapping and repulsing when the two polarons are close enough to each other. The overlap of wave functions leads to electron transition between states of level 99 (101) and level 100 (102) during the collision of the two polarons. We now analyze specifically the two cases in Fig. 7.

For a relatively weak electric field, the two polarons are accelerated to move with low velocities. Then the time it takes for the collision is long enough, about 150 fs, for electron transition. The inset of Fig. 7(a) shows that electron transition from the state of level 99 to that of level 100 and from level 101 to level 102 takes place simultaneously in an oscillation form during the collision. In the real space, the electric potential drop between the two polarons favors electron to transit from the left to the right to redistribute net charge. When the resultant charge changes sign, the lattice deformations of the two polarons begin to separate under the influence of electric field and move backward with a lower velocity. The velocity here is the saturation velocity for a polaronlike state and is determined by the amount of the resultant charge as well as by the strength of the electric

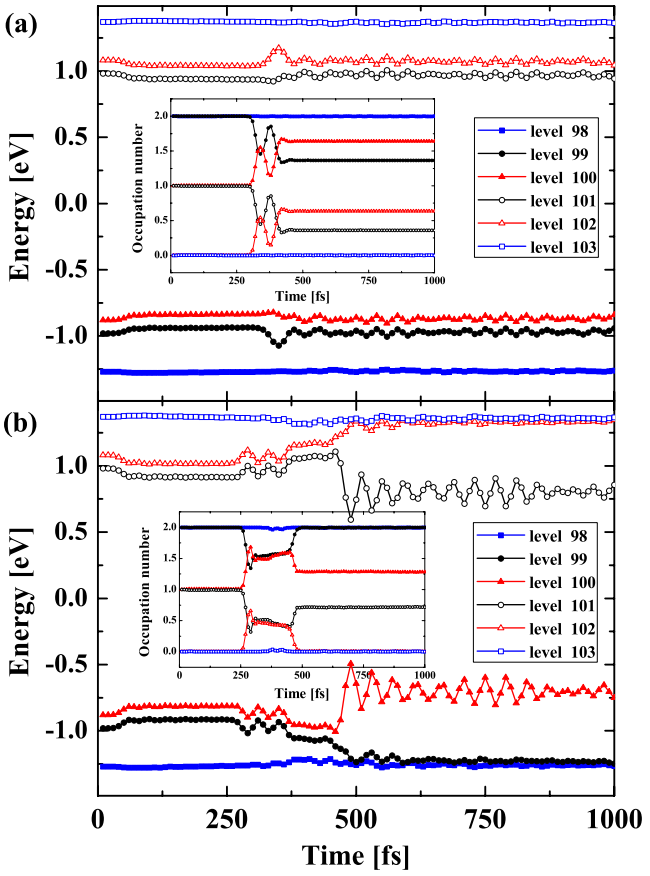

FIG. 7. (Color online) Time dependence of instantaneous eigenlevels of the chain described in Fig. 6: (a) $F=5.0\times10^5$ V/cm; (b) $F=1.0\times10^6$ V/cm. The insets are the temporal evolution of the occupation number of the corresponding levels.

field.[24,47] Thus, it is the electron transition between the two polarons that results in the paradox between Fig. 6(a) and Fig. 6(c) as stated above. After the collision, level 99 and level 101 hold a hole-polaron-like nonintegral occupation while level 100 and level 102 are partially occupied like an electron polaron. It implies that the products of the collision here are mixed states consisting of both polaron and exciton components. The polaron component can be identified by the amount of the resultant charge.

For a strong electric field, the two polarons are sufficiently accelerated. Then the time it takes for the first collision is too short, about 50 fs, to change sign of the resultant charge by electron transition. The repulsion between their wave functions rebounds the two polarons but they resume a second collision as a result of the drive of electric field. As the two polarons have been scattered into mixed states by the first collision [see the inset of Fig. 7(b)], the repulsion between their wave functions is accordingly reduced in the second collision and hence they merge directly to form a single larger lattice deformation. Two localized levels (level 99 and level 102) gradually merge into the continuum and the rest (level 100 and level 101) go deeper into the gap to form a self-trapping excitonlike neutral state, as shown in Fig. 7(b). Note that the excitonlike state is also a mixed state as the

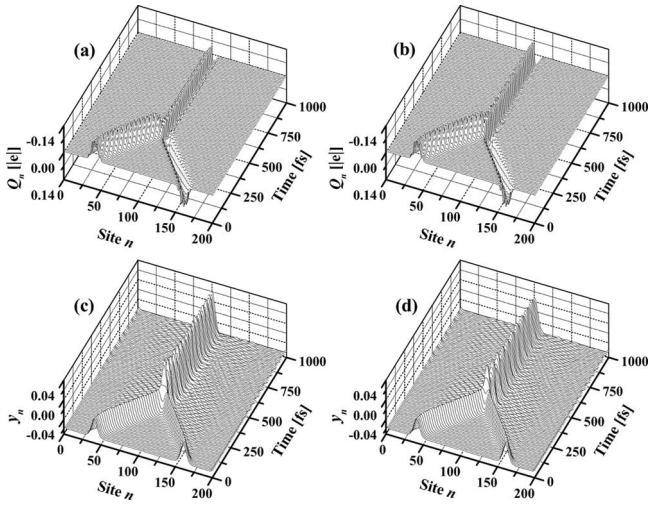

FIG. 8. Time dependence of Q_n and y_n of two oppositely charged polarons in a chain with (a), (c) $\Delta=0.4$ eV; (b), (d) $\Delta=0.6$ eV. The electric field is $F=5.0\times10^5$ V/cm. The unit of y_n is in angstrom.

occupation of level 100 and level 101 after the second collision is not for a full exciton, in which the two levels should be integrally occupied by one electron, respectively. It is due to the fact that part of the charge is scattered out into delocalized states of the continuum levels by the two collisions. This can be confirmed by the slight variation in the occupation number of level 98 and level 103 between the two collisions and also by the net charge fluctuation on the whole chain in Fig. 6(b).

As the collision products here are mixed states, the exciton component represents the probability of its formation in the collision process. Similar results were also observed in relevant studies in a homopolymer chain. In a detailed study of polaron recombination in Ref. 56 with a quantum molecular dynamics method,[57] it was demonstrated that the yield of singlet or triplet exciton, in terms of the scattering cross section, is variable and can be greatly enhanced if the excitonic state is nearly resonant with the incident polaron. Another study of polaron-pair scattering in Ref. 58 with the same method employed here discovered that the full degeneracy of polaron levels maximizes the repulsion between the two polarons in the collision and the exciton component after the scattering is field dependent. It is expected that with the increase in level offset, the probability of electron transition gradually diminishes. The repulsion between polarons in the collision weakens and eventually even becomes negligible when the level offset is large enough, e.g., exceeding the value of polaron binding energy.

b. $\varepsilon_b^p<\Delta<\varepsilon_b^{el}$. In Figs. 8(a) and 8(c), we present a chain with level offset of $\Delta=0.4$ eV at an electric field of 5.0×10^5 V/cm. The level offset is greater than the polaron binding energy but less than the exciton binding energy ε_b^{el}. For the lattice development [see Fig. 8(c)], the two polarons merge directly to form a self-trapping state with larger lattice deformation with respect to the polarons when they encounter each other at the interface. The evolution of the net

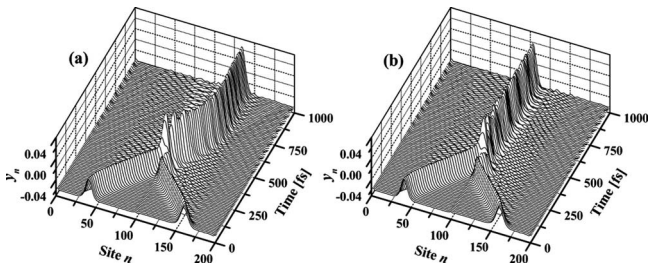

FIG. 9. Time dependence of y_n of two oppositely charged polarons in a chain with (a) $\Delta^-=0.28$ eV, $\Delta^+=0.52$ eV; (b) $\Delta^-=0.48$ eV, $\Delta^+=0.72$ eV. The electric field is $F=5.0\times10^5$ V/cm. The unit of y_n is in angstrom.

charge distribution [see Fig. 8(a)] reveals that the net charge localized in the self-trapping state markedly decreases but with a little polarization in the direction along the chain. By checking the evolution of the instantaneous eigenlevels (not shown), we find that level 100 and level 101 go correspondingly deeper into the gap to form localized levels of the self-trapping state and they are occupied nearly integrally as a full exciton. No signature of clear electron transition between states of the levels is observed in this process. It indicates that an exciton is created here with much greater probability than that in the case of $\Delta<\varepsilon_b^p$. It can be attributed to at least two factors. On the one hand, the interface blockage to the polarons' migration makes for their sufficient overlapping at the interface. On the other hand, the level offset eliminating the degeneracy of the polaronic levels is large enough to minimize the repulsion between the two polarons. More calculations with a wide range of electric fields show that this process is field independent. Therefore, it is clear that an exciton can be efficiently created by geminate combination of polarons in the presence of level offset with appropriate values.

The exciton created here consists of an electron and a hole. It is confined to the interface as both sides are barriers for the exciton migration. However, as the level offset is less than the exciton binding energy ε_b^{eI}, it is expected that the exciton is stable enough to overcome the barrier to enter any one of the two segments. To this end, we present in Fig. 9(a) the lattice development of a chain with unsymmetrical level offsets, that is $\Delta^-=0.4-0.12=0.28$ eV and $\Delta^+=0.4+0.12=0.52$ eV. It is obtained by reducing the energy gap of segment B by 0.24 eV. In calculations, we set $t'=0.8$ eV in segment B and hold other parameters fixed. One can see that an exciton is first created at the interface and then it overcomes the blockage of level offset Δ^- and migrates into segment B. As the exciton binding energy ε_b^{eI} is greater than Δ^- but less than Δ^+, the exciton enters segment B with much more possibility than segment A.

Thus, one can give a conclusion that for level offsets greater than the polaron binding energy but less than the exciton binding energy ε_b^{eI}, two oppositely charged polarons can combine directly and efficiently at the interface to create a full exciton. The exciton will not be confined to the interface but is stable enough to migrate freely in the whole

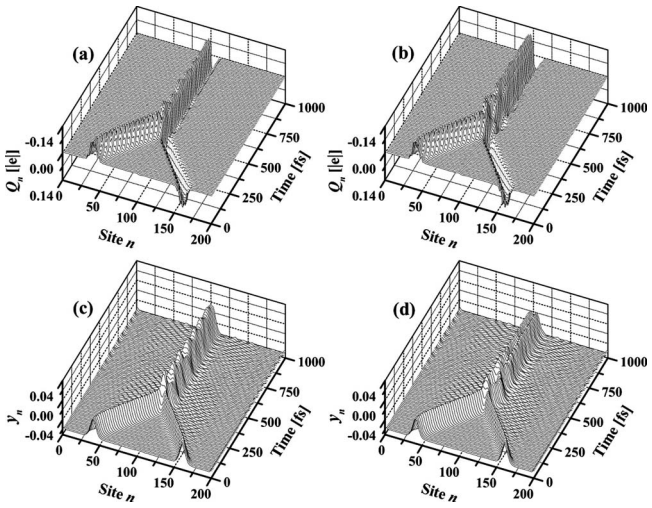

FIG. 10. Time dependence of Q_n and y_n of two oppositely charged polarons in a chain with (a), (c) $\Delta=0.75$ eV; (b), (d) $\Delta=0.85$ eV. The electric field is $F=5.0\times10^5$ V/cm. The unit of y_n is in angstrom.

chain. In view of this, at least for the intrachain process, it will be efficient to employ donor-acceptor copolymers with level offsets within this range for photo- or electroluminescent use in organic LEDs.

c. $\varepsilon_b^{eI}<\Delta<\varepsilon_b^{eII}$. We give in Figs. 8(b) and 8(d) a chain with level offset of $\Delta=0.6$ eV, a value between that of the two forms of exciton binding energy. The applied electric field is 5.0×10^5 V/cm. In comparison with Figs. 8(a) and 8(c), no difference is obtained but there is a more evident polarization of the net charge in the exciton [see Fig. 8(b)] and a little decrease in magnitude of the exciton lattice deformation [see Fig. 8(d)]. By further increasing the level offset, such as $\Delta=0.75$ eV shown in Figs. 10(a) and 10(c), one can get a similar result but with further polarization of the net charge and the magnitude of the exciton lattice deformation decreases more. This process is also field independent.

The results indicate that a level offset greater than ε_b^{eI} cannot prevent two polarons from combining to form an exciton, though ε_b^{eI} is the lowest energy supplied to an exciton to create a pair of free polarons in a homopolymer chain or a heterojunction.[30] In other words, the level offset here is not large enough to split the exciton. To explore the role ε_b^{eI} plays in the combination process, we reduce the energy gap of segment B by 0.24 eV to make $\Delta^-=0.6-0.12=0.48$ eV and $\Delta^+=0.6+0.12=0.72$ eV. Then we obtain unsymmetrical level offsets with both Δ^- and Δ^+ greater than ε_b^{eI}. Quite different from the case in Fig. 9(a), it is shown in Fig. 9(b) that the exciton is confined to the interface throughout the evolution. Simulations with disturbances, such as introducing lattice fluctuations in segment A, also give results that the exciton resides stably at the interface rather than enter segment B. It is clear that the exciton binding energy ε_b^{eI} with respect to the level offset plays a major role in determining exciton migration rather than dissociation in the copolymer chain.

Therefore, one can conclude that for level offsets with

magnitudes between that of the two forms of exciton binding energy, an exciton can also be created by geminate combination of oppositely charged polarons. However, the created exciton is just confined to the interface and hardly migrates freely in the copolymer chain.

d. $\Delta > \varepsilon_b^{eII}$. A chain with level offset of $\Delta=0.85$ eV, greater than the exciton binding energy ε_b^{eII}, is depicted in Figs. 10(b) and 10(d). One can see from the lattice development in Fig. 10(d) that the two polarons at the interface undergo a succession of mergence and fission and eventually form a polaron pair with two peaks in the lattice deformation. The great interfacial polarization of the net charge distribution in Fig. 10(b) also reveals that the state at the interface is not an exciton. Similar field-independent results are also observed for other magnitudes within $\Delta > \varepsilon_b^{eII}$ and the two polarons are completely separated if the level offset is large enough.

It indicates that an exciton cannot survive at the interface if the level offset is greater than the exciton binding energy ε_b^{eII} instead of ε_b^{eI}, quite different from the case of exciton fission in the interchain process.[30] We expect that the difference arises mainly from the flexibility of the intrachain interface with large transfer integral with respect to the interchain interface of weak coupling. Here, the self-adjustment of interfacial bond length through electron-lattice coupling in the process of exciton formation and relaxation can reduce effectively the total energy of the system and render the exciton more stable relative to that in the interchain case. However, the energy reduction through interfacial self-adjustment is finite and with an upper limit of the difference between the two forms of exciton binding energy.

Therefore, one can also arrive at a conclusion that for level offsets greater than the exciton binding energy ε_b^{eII}, two oppositely charged polarons cannot combine to create an exciton but form an intrachain polaron pair divided by the interface. In other words, an exciton at the interface is not the lowest-energy state and will fiss to form intrachain charge-separated state. Thus, it is expected that donor-acceptor copolymers for photovoltaic application will be efficient if the level offsets are designed in this way.

One should note from Figs. 8 and 10 that with the increase in level offset, the polarization of the exciton is enhanced and the magnitude of the exciton lattice deformation is reduced. To explicitly reveal this behavior, we study the evolution of the total net charge of the two segments and the electric dipole moment $\vec{P}(\tau)$ of the chain defined as

$$\vec{P}(\tau) = \sum_n \vec{i}(na + u_n)q_n(\tau), \tag{22}$$

where $\vec{i}$ is the unit vector in the coordinate space. To sum $q_n(\tau)$ over the sites in one segment, one can get the corresponding total net charge. The results are given in Fig. 11. The inset shows that for all cases the total net charge is negative in segment A and positive in segment B, indicating that all the electric dipole moments are directed from A to B, opposite to the direction of the external electric field. It is clear that the polarization of the exciton is induced by the level offset at the interface rather than by the electric field.[59] Note that the oscillation of $\vec{P}(\tau)$ in Fig. 11 harmonizes with the lattice development of the corresponding exciton, especially with the periodic fluctuation of the deformation peak. The decrease in magnitude of the exciton lattice deformation results mainly from the polarization which diminishes the total force exerted to each site by the electron and the hole through electron-lattice coupling. In view of the fact that the polarized exciton created in Sec. III B 1 c, especially for Δ close to ε_b^{eII}, is confined to the interface, not inclined to be fissed, and likely nonradiative, it is expected that the exciton will hardly contribute to the efficiency in both photovoltaic and LEDs use.

2. Effects of interfacial coupling and e-e interaction

As already schematically shown in the inset of Fig. 4, a weak (strong) coupling introduces an additional energy Δ_{add} to the interface to create a barrier (well). We now consider the effect of interfacial coupling on the process of geminate combination.

A chain with level offset of $\Delta=0.6$ eV and interfacial coupling of $\beta=0.9$ is presented in Figs. 12(a) and 12(c). The behavior here differs from the case of $\Delta=0.6$ eV in Figs. 8(b) and 8(d) but resembles the case of $\Delta=0.85$ eV in Figs. 10(b) and 10(d). It is due to the fact that Δ here is replaced by an effective level offset of $\Delta+\Delta_{add}$, greater than the exciton binding energy ε_b^{eII}, and then the evolution of the system accords with the description for $\Delta > \varepsilon_b^{eII}$.

On the other hand, a chain with level offset of $\Delta=0.85$ eV and interfacial coupling of $\beta=1.1$ is depicted in Figs. 12(b) and 12(d). Although the effective level offset $\Delta+\Delta_{add}$ is much greater than ε_b^{eII}, an exciton can also be formed at the interface by partially trapping the electron and the hole in the well created by the strong interfacial coupling. Note in Fig. 12(b) that a little amount of net charge is trapped by interface electronic states from the beginning of the evolution, and the exciton is also polarized due to the presence of level offset. It can be expected that an interface with strong coupling can serve as a trap center for excitons and may have negative impacts on photovoltaic applications.

One should note from the beginning of the simulations in Figs. 12(c) and 12(d) that a small magnitude of lattice deformation is created at the interface. The little deformations here actually represent the interfacial bond length variation as a result of the weak and strong interfacial coupling, respectively. By analyzing the relation between y_n and the bond length, it is found that for the weak coupling in Fig. 12(c), a larger absolute value of y_n at the interface corresponds to the increase in the interfacial bond length. On the contrary, the strong coupling in Fig. 12(d) gives rise to the reduction in the bond length. It accords with the argument of bond length variation presented in Sec. III A. For the lattice development, the little deformations can visualize the effect of the barrier (well) that divides (traps) the two polarons at the interface.

Therefore, one can conclude that the interfacial coupling can dramatically affect the geminate combination of oppo-

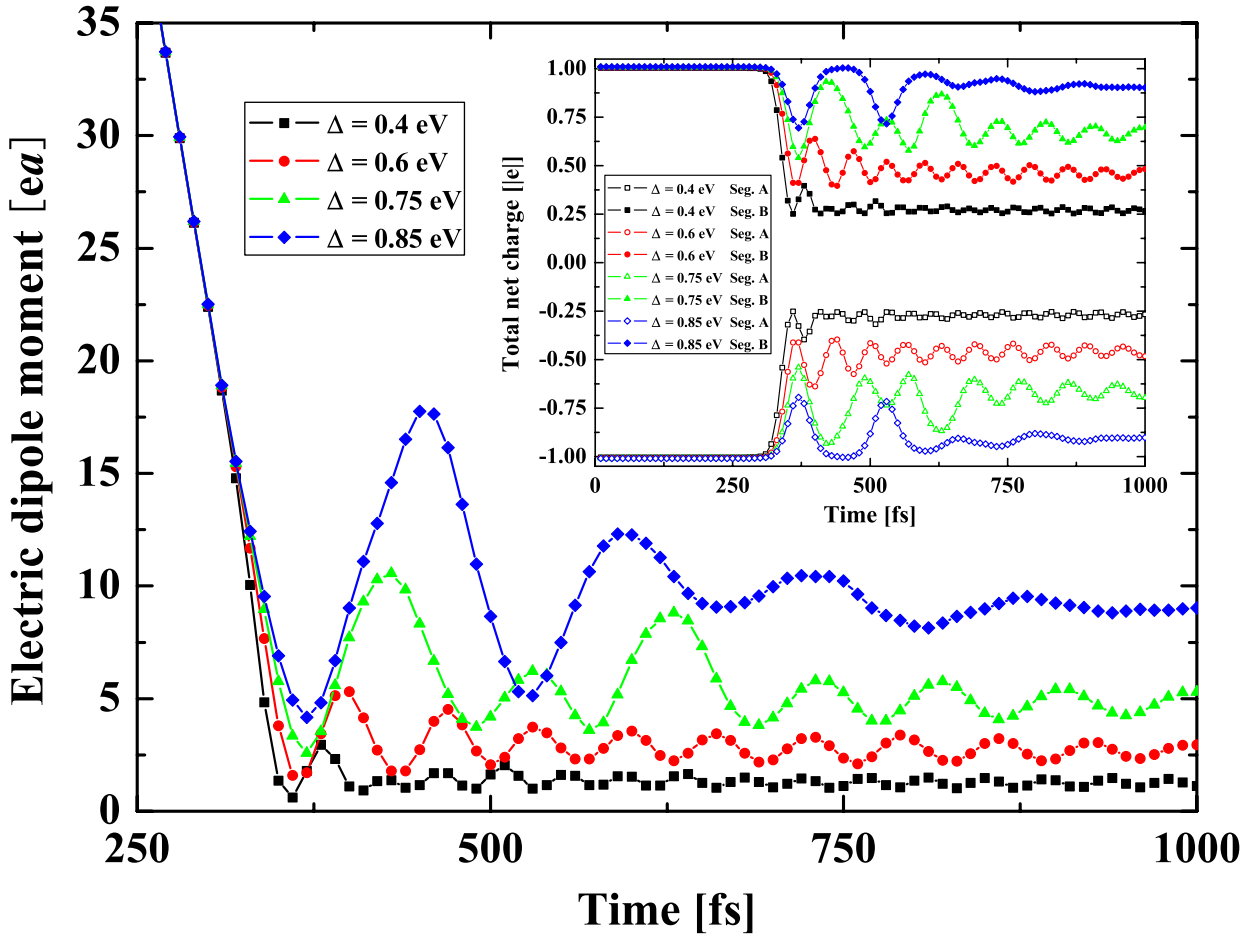

FIG. 11. (Color online) Time dependence of the electric dipole moment in chains described in Figs. 8 and 10. The inset is the temporal evolution of the total net charge of the two segments.

sitely charged polarons. Interfacial coupling can be as important as level offset in impacting on the intrachain process in donor-acceptor copolymers.

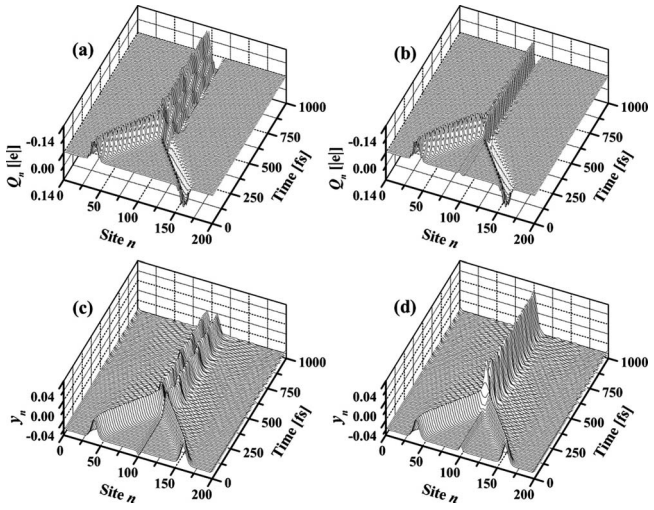

FIG. 12. Time dependence of Q_n and y_n of two oppositely charged polarons in a chain with (a), (c) $\Delta=0.6$ eV, $\beta=0.9$; (b), (d) $\Delta=0.85$ eV, $\beta=1.1$. The electric field is $F=5.0\times10^5$ V/cm. The unit of y_n is in angstrom.

It should be stressed that *e-e* interactions have important influence on polarons and excitons in conjugated polymers. We consider this effect by employing the Hubbard model[60] to give a brief discussion.

$$H_{e\text{-}e}=\frac{U}{2}\sum_n c^{\dagger}_{n,\uparrow}c_{n,\uparrow}c^{\dagger}_{n,\downarrow}c_{n,\downarrow}, \tag{23}$$

where U is the on-site repulsion between electrons with spin up and spin down.

Figure 13 depicts the dependence of polaron and exciton binding energy on U. For a triplet exciton, in which two open shell electrons with the same spin coexist, the two forms of exciton binding energy is enhanced quickly by increasing U. However, for singlet manifold with two open shell electrons of opposite spins, the exciton binding energy ε_b^{eI} gradually decreases whereas ε_b^{eII} keeps constant with the increase in U. Similar behavior of different dependence of ε_b^{eI} on U in the two manifolds was also obtained by another theoretical study on excitons in conjugated polymers.[61] The reduction in ε_b^{eI} with U for the singlet exciton is mainly ascribed to the Coulomb repulsion between the two oppositely spin-orientated electrons therein. For the triplet exciton and the polaron, where two noninteracting electrons and one open shell electron are confined, respectively, the on-site repulsion gives

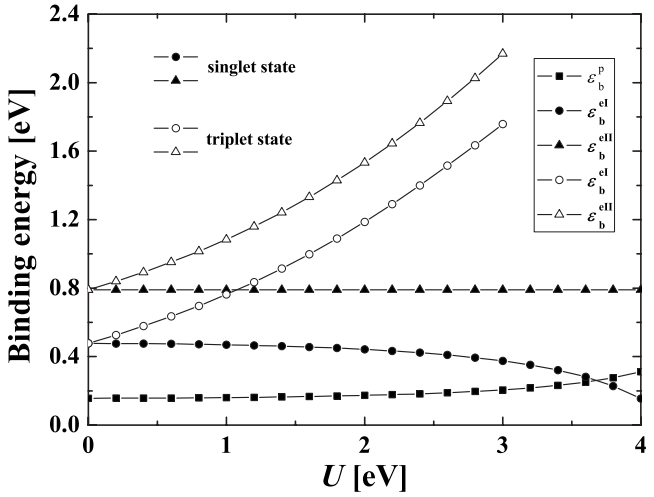

FIG. 13. Polaron and exciton binding energy versus U.

rise to depression of the dimerization of the lattice, as pointed out in Ref. 62 for a short-range interaction with strong screening. It enhances in effect the lattice deformations of the triplet exciton and the polaron, and accordingly enhances their binding energies. As the polaron binding energy is independent of the manifold of the chain, there exists a compensation balance between ε_b^{eI} and ε_b^{eII} according to Eq. (21). Then we obtain different dependence of ε_b^{eII} on U in the two manifolds.

In Fig. 14, we present chains in singlet state with different on-site repulsions. For the lattice development [see Figs. 14(c) and 14(d)], the magnitude of the exciton deformation is gradually damped in the evolution and the damping is enhanced by a larger U. Correspondingly, the polarized net charge in the exciton deformation fluctuates violently and is even scattered out to spread widely in the rest of the chain for the larger U case [see Figs. 14(a) and 14(b)]. It indicates

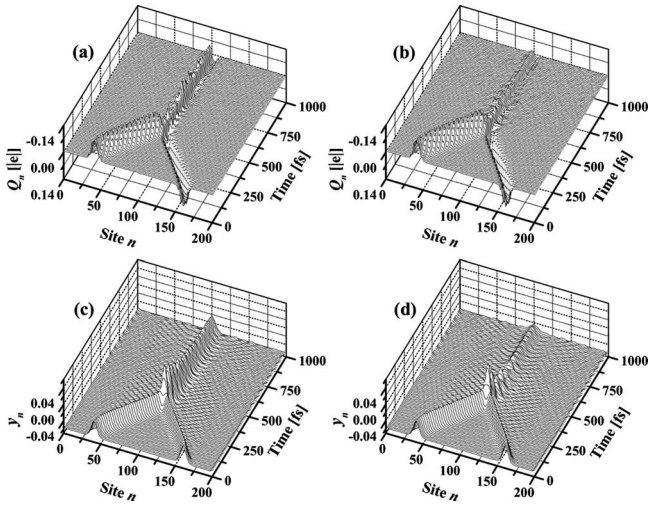

FIG. 14. Time dependence of Q_n and y_n of two oppositely charged polarons in chains with (a), (c) $U=1.0$ eV; (b), (d) $U=2.0$ eV. The molecules are in singlet state. The level offset is $\Delta=0.4$ eV. The electric field is $F=5.0\times10^5$ V/cm. The unit of y_n is in angstrom.

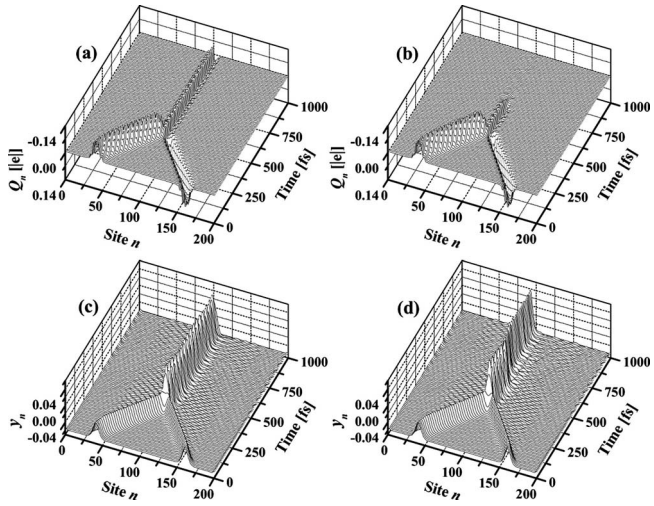

FIG. 15. Time dependence of Q_n and y_n of two oppositely charged polarons in chains with (a), (c) $U=1.0$ eV; (b), (d) $U=2.0$ eV. The molecules are in triplet state. The level offset is $\Delta=0.4$ eV. The electric field is $F=5.0\times10^5$ V/cm. The unit of y_n is in angstrom.

that a singlet exciton is less stable with the increase in U and can relax to a lower-energy state by interacting with the lattice.

On the other hand, for chains in triplet state shown in Fig. 15, the excitons are much stable with lattice deformations larger than that in Fig. 8(c) in the absence of on-site repulsion. Note in Figs. 15(b) and 15(d) that the exciton is so stable, with ε_b^{eI} about 1.2 eV, that it migrates from the interface into segment A at about $\tau=750$ fs in the relaxation process, accompanying the disappearance of the net charge polarization in the exciton.

It has been demonstrated in MEH-PPV that triplet states are much more strongly bound and energetically stable than singlet states and so are less perturbed by other effects.[63] It has also been estimated experimentally in PPV that the lowest-lying singlet exciton is about 0.3–0.4 eV below the conductivity threshold of the free polaron pair[64,65] and the lowest-lying triplet state lies about 0.9 eV lower than the singlet state.[66] It accords well with the exciton binding energy ε_b^{eI} in Fig. 13 at about $U=2.2$ eV, where for singlet state $\varepsilon_b^{eI}=0.43$ eV and for triplet state $\varepsilon_b^{eI}=1.29$ eV. Thus, the stability of excitons with the two manifolds can be dramatically affected by the e-e interaction considered here.

IV. SUMMARY AND CONCLUDING REMARKS

In summary, we have presented a model study of polaron motion and geminate combination in a molecular chain of donor-acceptor copolymers. The simulations are performed by using an extended version of the one-dimensional SSH model. In particular, we mainly focus on two factors impacting on the intrachain process, i.e., level offset and interfacial coupling. A general rule associated with the ratio of level offset to polaron or exciton binding energy is suggested to contribute to optimizing donor-acceptor copolymers for LEDs or photovoltaic use. According to the rule, we identify

two cases for polaron motion and four cases for geminate combination of oppositely charged polarons.

It is found for polaron motion that, if the polaron binding energy is greater than the level offset, a polaron can cross the interface only if the electric field is strong enough. On the other hand, if the level offset is greater than the polaron binding energy, a polaron, as an entity consisting of both charge and lattice deformation, cannot cross the interface regardless of the strength of electric field. It is also suggested that the polaron binding energy should be calculated by the total energy of the system including both the electronic and the lattice part, rather than only by the electronic energy. The result can qualitatively explain some experimental measurements on conductivity of copolymers.

For geminate combination of polarons, if $\Delta < \varepsilon_b^p$, the products of the combination are mixed states and the process is field dependent. This behavior resembles closely the results of other studies on polaron collision in homopolymers. If $\varepsilon_b^p < \Delta < \varepsilon_b^{eI}$, two polarons can combine directly and efficiently at the interface to create a full exciton. The exciton is stable enough to migrate freely in the whole chain. If $\varepsilon_b^{eI} < \Delta < \varepsilon_b^{eII}$, the created exciton, more accurately an intrachain polarized exciton, is just confined to the interface and can hardly migrate in the chain. And if $\Delta > \varepsilon_b^{eII}$, two polarons cannot combine to create an exciton but form an intrachain polaron pair divided by the interface as the lowest-energy state. It is determined by the flexibility of the intrachain interface with large transfer integral that both the two forms of exciton binding energy are of importance to the combination process. It is expected to employ efficiently donor-acceptor copolymers with $\varepsilon_b^p < \Delta < \varepsilon_b^{eI}$ for LEDs use and with $\Delta > \varepsilon_b^{eII}$ in photovoltaic application.

We further study the effect of interfacial coupling. It is found that an interface with weak coupling serves as an energy barrier and that with strong coupling as a well. Interfacial coupling can be as important as level offset in impacting on the polaron motion and geminate combination in donor-acceptor copolymers. The effect of *e-e* interactions is also briefly discussed by employing the Hubbard model. It is found that a triplet exciton is much more energetically stable than a singlet one in the presence of on-site repulsions. This can be explained by the exciton binding energy and accords well with relative experiments.

Finally, we remark that this simulation has been focused academically on a specific case with idealized conditions in donor-acceptor copolymers. The conclusion is applicable for samples where intrachain process dominates or works. A theory that widely holds true in real materials needs further verifying by addressing some realistic effects, e.g., the conjugation length, the order degree of molecules, and the temperature. We believe that, together with the relevant study of interchain process by other authors, the underlying physics revealed here is helpful in guiding experiments in donor-acceptor polymer operations.

ACKNOWLEDGMENTS

The authors would like to give special thanks to H. Cohen for his much appreciated comments toward this manuscript. Financial support from the National Natural Science Foundation of China (Grant No. 10574082) and the Natural Science Foundation of Shandong Province (Grant No. Z2005A01) is gratefully acknowledged.

*To whom correspondence should be addressed.liuds@sdu.edu.cn

[1] R. H. Friend, R. W. Gymer, A. B. Holmes, J. H. Burroughes, R. N. Marks, C. Taliani, D. D. C. Bradley, D. A. Dos Santos, J. L. Brédas, M. Lögdlund, and W. R. Salaneck, Nature (London) **397**, 121 (1999).

[2] A. Dodabalapur, H. E. Katz, L. Torsi, and R. C. Haddon, Science **269**, 1560 (1995).

[3] G. Yu, J. Gao, J. C. Hummelen, F. Wudl, and A. J. Heeger, Science **270**, 1789 (1995).

[4] J. H. Burroughes, D. D. C. Bradley, A. R. Brown, R. N. Marks, K. Mackay, R. H. Friend, P. L. Burns, and A. B. Holmes, Nature (London) **347**, 539 (1990).

[5] P. L. Burn, A. B. Holmes, A. Kraft, D. D. C. Bradley, A. R. Brown, R. H. Friend, and R. W. Gymer, Nature (London) **356**, 47 (1992).

[6] H. J. Brouwer, A. Hilberer, V. V. Krasnikov, M. Werts, J. Wildeman, and G. Hadziioannou, Synth. Met. **84**, 881 (1997).

[7] T. P. Nguyen, L. C. Chen, X. Wang, and Z. Huang, Opt. Mater. **9**, 154 (1998).

[8] J. I. Lee, T. Zyung, R. D. Miller, Y. H. Kim, S. C. Jeoung, and D. Kim, J. Mater. Chem. **10**, 1547 (2000).

[9] E. E. Neuteboom, S. C. J. Meskers, P. A. van Hal, J. K. J. van Duren, E. M. Meijer, R. A. J. Janssen, H. Dupin, G. Pourtois, J. Cornil, R. Lazzaroni, J. L. Brédas, and D. Beljonne, J. Am. Chem. Soc. **125**, 8625 (2003).

[10] H. Aarnio, M. Westerling, R. Osterbacka, M. Svensson, M. R. Andersson, and H. Stubb, Chem. Phys. **321**, 127 (2006).

[11] C. J. Shi, Y. Yao, Y. Yang, and Q. B. Pei, J. Am. Chem. Soc. **128**, 8980 (2006).

[12] H. A. Klok and S. Lecommandoux, Adv. Mater. (Weinheim, Ger.) **13**, 1217 (2001).

[13] J. S. Kim, Pure Appl. Chem. **74**, 2031 (2002).

[14] A. K. Bakhshi and P. Bhargava, J. Chem. Phys. **119**, 13159 (2003).

[15] E. M. Conwell, H. Y. Choi, and S. Jeyadev, Synth. Met. **49**, 359 (1992).

[16] A. Johansson and S. Stafström, Phys. Rev. Lett. **86**, 3602 (2001).

[17] M. A. Loi, S. Toffanin, M. Muccini, M. Forster, U. Scherf, and M. Scharber, Adv. Funct. Mater. **17**, 2111 (2007).

[18] H. W. Wang, Y. J. Cheng, C. H. Chen, T. S. Liu, W. Fann, C. L. Lin, Y. P. Chang, K. C. Liu, and T. Y. Luh, Macromolecules **40**, 2666 (2007).

[19] Q. L. Song, C. M. Li, M. B. Chan-Park, M. Lu, H. Yang, and X. Y. Hou, Phys. Rev. Lett. **98**, 176403 (2007).

[20] V. I. Arkhipov, P. Heremans, and H. Bässler, Appl. Phys. Lett.

82, 4605 (2003).
[21] S. Gunes, H. Neugebauer, and N. S. Sariciftci, Chem. Rev. (Washington, D.C.) **107**, 1324 (2007).
[22] S. A. Jenekhe and X. L. Chen, Science **279**, 1903 (1998).
[23] S. V. Rakhmanova and E. M. Conwell, Appl. Phys. Lett. **75**, 1518 (1999).
[24] A. A. Johansson and S. Stafström, Phys. Rev. B **69**, 235205 (2004).
[25] X. J. Liu, K. Gao, J. Y. Fu, Y. Li, J. H. Wei, and S. J. Xie, Phys. Rev. B **74**, 172301 (2006).
[26] S. A. Jenekhe, L. Lu, and M. M. Alam, Macromolecules **34**, 7315 (2001).
[27] M. Tong, C. X. Sheng, C. Yang, Z. V. Vardeny, and Y. Pang, Phys. Rev. B **69**, 155211 (2004).
[28] S. Karabunarliev and E. R. Bittner, J. Phys. Chem. B **108**, 10219 (2004).
[29] M. Westerling, H. Aarnio, R. Österbacka, H. Stubb, S. M. King, A. P. Monkman, M. R. Andersson, K. Jespersen, T. Kesti, A. Yartsev, and V. Sundström, Phys. Rev. B **75**, 224306 (2007).
[30] E. R. Bittner, J. G. S. Ramon, and S. Karabunarliev, J. Chem. Phys. **122**, 214719 (2005).
[31] E. L. Frankevich, A. A. Lymarev, I. Sokolik, F. E. Karasz, S. Blumstengel, R. H. Baughman, and H. H. Horhold, Phys. Rev. B **46**, 9320 (1992).
[32] C. H. Lee, G. Yu, D. Moses, and A. J. Heeger, Phys. Rev. B **49**, 2396 (1994).
[33] J. M. Leng, S. Jeglinski, X. Wei, R. E. Benner, Z. V. Vardeny, F. Guo, and S. Mazumdar, Phys. Rev. Lett. **72**, 156 (1994).
[34] R. N. Marks, J. J. M. Halls, D. D. C. Bradley, R. H. Friend, and A. B. Holmes, J. Phys.: Condens. Matter **6**, 1379 (1994).
[35] I. H. Campbell, T. W. Hagler, D. L. Smith, and J. P. Ferraris, Phys. Rev. Lett. **76**, 1900 (1996).
[36] S. Barth and H. Bassler, Phys. Rev. Lett. **79**, 4445 (1997).
[37] E. M. Conwell, Synth. Met. **83**, 101 (1996).
[38] M. Hultell and S. Stafström, Phys. Rev. B **75**, 104304 (2007).
[39] W. P. Su, J. R. Schrieffer, and A. J. Heeger, Phys. Rev. Lett. **42**, 1698 (1979); Phys. Rev. B **22**, 2099 (1980).
[40] D. S. Liu, L. M. Mei, S. J. Xie, and S. H. Han, J. Phys.: Condens. Matter **12**, 4333 (2000).
[41] S. J. Xie, L. M. Mei, and D. L. Lin, Phys. Rev. B **50**, 13364 (1994).
[42] K. Gao, X. J. Liu, D. S. Liu, and S. J. Xie, Phys. Rev. B **75**, 205412 (2007).
[43] H. W. Streitwolf, Phys. Rev. B **58**, 14356 (1998).
[44] R. W. Brankin, I. Gladwell, and L. F. Shampine, RKSUITE: Software for ODE IVPS, http://www.netlib.org
[45] Y. Li, X. J. Liu, J. Y. Fu, D. S. Liu, S. J. Xie, and L. M. Mei, Phys. Rev. B **74**, 184303 (2006).
[46] A. J. Heeger, S. Kivelson, J. R. Schrieffer, and W. P. Su, Rev. Mod. Phys. **60**, 781 (1988).
[47] D. M. Basko and E. M. Conwell, Phys. Rev. Lett. **88**, 056401 (2002).
[48] K. D. Meisel, H. Vocks, and P. A. Bobbert, Phys. Rev. B **71**, 205206 (2005).
[49] M. Taniguchi and T. Kawai, Phys. Rev. E **72**, 061909 (2005).
[50] I. I. Fishchuk, V. I. Arkhipov, A. Kadashchuk, P. Heremans, and H. Bässler, Phys. Rev. B **76**, 045210 (2007).
[51] T. Kreouzis, D. Poplavskyy, S. M. Tuladhar, M. Campoy-Quiles, J. Nelson, A. J. Campbell, and D. D. C. Bradley, Phys. Rev. B **73**, 235201 (2006).
[52] C. Q. Wu, Y. Qiu, Z. An, and K. Nasu, Phys. Rev. B **68**, 125416 (2003).
[53] H. A. Mizes and E. M. Conwell, Synth. Met. **68**, 145 (1995).
[54] V. W. L. Lim, E. T. Kang, K. G. Neoh, Z. H. Ma, and K. L. Tan, Appl. Surf. Sci. **181**, 317 (2001).
[55] C. C. Han, S. P. Hong, K. F. Yang, M. Y. Bai, C. H. Lu, and C. S. Huang, Macromolecules **34**, 587 (2001).
[56] M. N. Kobrak and E. R. Bittner, Phys. Rev. B **62**, 11473 (2000).
[57] M. N. Kobrak and E. R. Bittner, J. Chem. Phys. **112**, 5399 (2000); **112**, 5410 (2000).
[58] Z. An and C. Q. Wu, Synth. Met. **137**, 1151 (2003).
[59] R. L. Fu, G. Y. Guo, and X. Sun, Phys. Rev. B **62**, 15735 (2000).
[60] J. Hubbard, Proc. R. Soc. London, Ser. A **276**, 238 (1963).
[61] S. Abe, J. Yu, and W. P. Su, Phys. Rev. B **45**, 8264 (1992).
[62] C. Q. Wu, X. Sun, and K. Nasu, Phys. Rev. Lett. **59**, 831 (1987).
[63] A. P. Monkman, H. D. Burrows, M. da G. Miguel, I. Hamblett, and S. Navaratnam, Chem. Phys. Lett. **307**, 303 (1999).
[64] S. F. Alvarado, P. F. Seidler, D. G. Lidzey, and D. D. C. Bradley, Phys. Rev. Lett. **81**, 1082 (1998).
[65] J. L. Brédas, J. Cornil, and A. J. Heeger, Adv. Mater. (Weinheim, Ger.) **8**, 447 (1996).
[66] R. Osterbacka, M. Wohlgenannt, D. Chinn, and Z. V. Vardeny, Phys. Rev. B **60**, R11253 (1999).